

^{166}Er Mössbauer study of magnetic ordering in Er_3Ge_4 D. H. Ryan,¹ J. M. Cadogan,² and R. Gagnon¹¹*Physics Department and Centre for the Physics of Materials, McGill University, 3600 University Street, Montreal, Quebec, Canada H3A 2T8*²*School of Physics, The University of New South Wales, Sydney, NSW 2052, Australia*

(Received 12 December 2002; revised manuscript received 23 January 2003; published 10 July 2003)

^{166}Er Mössbauer spectroscopy has been used to study the magnetic ordering of erbium moments in Er_3Ge_4 . We find that the average Er moment is less than 80% of its free-ion value, and we have confirmed that at 1.5 K, the moment associated with Er atoms on the $4c$ site is 15% smaller than that on the $8f$ site. The hyperfine field at the $4c$ site declines much more rapidly with increasing temperature than that at the $8f$ site, however our data show no indication of the spin re-orientation claimed to occur at ~ 4 K.

DOI: 10.1103/PhysRevB.68.014413

PACS number(s): 75.50.Ee, 76.80.+y

I. INTRODUCTION

X-ray¹ and neutron² diffraction studies of Er_3Ge_4 have shown that it adopts an orthorhombic structure (Cmcm, space group #63) with two Er sites [$\text{Er}_1(8f)$, $\text{Er}_2(4c)$] and three Ge sites. Analysis of neutron diffraction data below the Néel temperature (T_N) of 7.3 K revealed a two-dimensional canted antiferromagnetic triangular structure with very different moments associated with the two crystallographically distinct Er sites. At 1.5 K these were reported to be $7.32(5) \mu_B/\text{Er}$ at the $\text{Er}_1(8f)$ site, and $6.37(6) \mu_B/\text{Er}$ at the $\text{Er}_2(4c)$ site.² In addition, distinct temperature dependences were found for the two Er sites, with the Er- $4c$ moment falling much more rapidly than the Er- $8f$ moment. Finally, a weak ($\sim 1^\circ$) spin reorientation was claimed to occur at the $8f$ site around 4 K associated with a slight change in the temperature dependence of the Er- $4c$ moment.

Two calorimetric studies of Er_3Ge_4 have been made.^{3,4} Janssen *et al.*³ reported a sharp peak at 6.9 K, corresponding to T_N and a weak shoulder around 4 K which they associated with the spin reorientation seen by neutron scattering. They commented that their integrated magnetic entropy is rather low, but their heat capacity for Er_3Ge_4 lies far below that reported by the same group for the non-magnetic analogue Lu_3Ge_4 .⁵ By contrast, a more recent calorimetric study⁴ revealed two clear features in the low-temperature heat capacity. The upper one (~ 7 K) is clearly associated with the onset of antiferromagnetic order, while a second peak at ~ 3.5 K was linked to the spin reorientation at 4 K reported in the neutron diffraction study.² While the total entropy change below T_N appears quite reasonable, the entropy associated with the 3.5-K peak is remarkably large, accounting for about a third of the total entropy change observed between 0 K and T_N (7.3 K). The size of the peak at ~ 3.5 K suggests either the presence of a magnetic impurity (which would bring it more into line with the earlier work³), or that far more than just a 1° spin reorientation occurs at 3.5 K in Er_3Ge_4 .

Given the inconsistencies between the two calorimetric studies, and the mismatch between the thermal and neutron diffraction signatures of the event at 3.5 K, we felt that a more local and direct study of the intrinsic magnetic ordering behavior was needed. We report the results of a ^{166}Er Möss-

bauer investigation of Er_3Ge_4 . The Er moments on the two sites are significantly reduced from the free ion $9 \mu_B/\text{Er}$, in full agreement with the neutron diffraction data.² We clearly resolve the moment difference between the two Er sites, and confirm their very different temperature dependences. However, neither our bulk characterization nor our microscopic measurements yield any significant indication of the magnetic changes claimed to occur below T_N .

II. EXPERIMENTAL METHODS

Samples were prepared in a triarc furnace with a base pressure of better than 6×10^{-7} mbar. Stoichiometric amounts of the pure elements [Er (99.9%) and Ge (99.999%)] were melted several times under pure (less than 1 ppm impurity) argon to ensure homogeneity. The ingot was then annealed under vacuum at 800°C for three weeks and water quenched.

Powder x-ray diffraction measurements were made at ambient temperature using $\text{Cu } K_\alpha$ radiation and analyzed using GSAS Ref. 6 to extract lattice parameters and check for impurities. Data for the specific sample used in this study are shown in Fig 1. Analysis confirms that this sample is primarily composed of the orthorhombic Er_3Ge_4 phase, with a ~ 5 wt.% ErGe impurity.

Basic magnetic characterization was carried out on a Quantum Design Physical Properties Measurement System (PPMS) susceptometer/magnetometer at temperatures from 1.8 K to room temperature. ac Susceptibility (χ_{ac}) measurements were made with a driving field of 1 mT at 137 Hz. Magnetization measurements were made in fields of up to 6 T.

Mössbauer measurements were obtained using 1 GBq ^{166}Ho sources prepared by neutron-activation of $\text{Ho}_{0.6}\text{Y}_{0.4}\text{H}_2$ in the SLOWPOKE reactor at Ecole Polytechnique, Montréal. The spectrometer was operated vertically with both source and sample cooled in a helium-flow cryostat and gave a linewidth of 2.5 mm/s (half width at half maximum) for an ErFe_2 standard at 4.5 K. Independent temperature control of the source was used to keep it at or above 5 K to avoid relaxation-induced line broadening which we have observed at lower source temperatures. A He/Ne laser interferometer was used to provide simultaneous calibration of all spectra. With the spectrometer operated in the sine mode, at a V_{max}

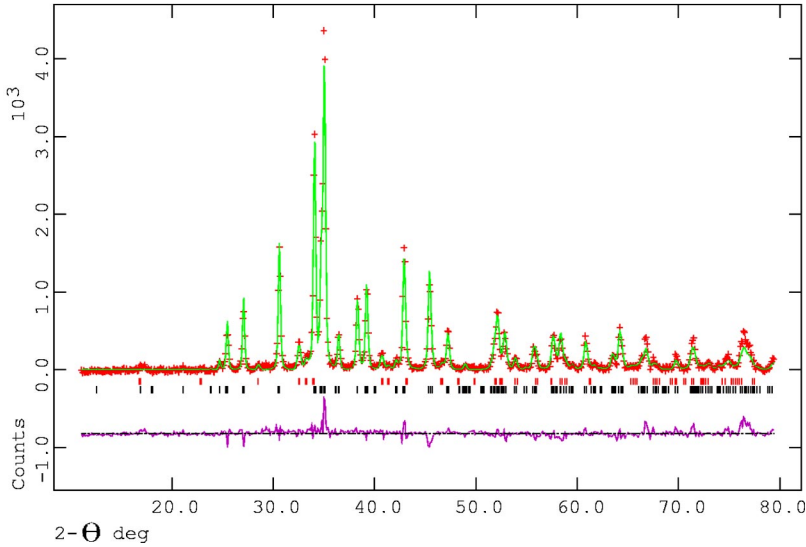


FIG. 1. (Color online) Cu- K_{α} x-ray diffraction pattern for Er_3Ge_4 with fit showing Er_3Ge_4 primary phase (lower markers) and ~ 5 -wt. % ErGe impurity (upper markers).

of ~ 82 mm/s, the calibration drift in V_{max} was less than 0.02 mm/s. The velocity calibration was cross checked using ErFe_2 .⁷

The spectra below 2.5 K could be fitted using a conventional nonlinear least-squares minimization routine with line positions and intensities derived from a full solution to the nuclear Hamiltonian for the ^{166}Er $2 \rightarrow 0$ transition. The hyperfine fields at 1.5 K yielded the moment ratio for the two Er sites, allowed a direct comparison with the Er moments deduced from neutron diffraction data, and provided confirmation of the field to moment scaling factor. The full Hamiltonian fits were also used to check the static limits of the fitting procedures employed for spectra obtained at higher temperatures where relaxation effects became increasingly important.

Slow electronic relaxation effects are ubiquitous in ^{166}Er Mössbauer spectra, occurring in both oxides⁸ and alloys.⁹ Er_3Ge_4 is no exception, with the lines broadening and collapsing towards the center with increasing temperature. Several strategies exist for dealing with such behavior. Our primary interest here is to obtain average hyperfine fields for the two Er sites for comparison with neutron diffraction. The observed hyperfine field in a Mössbauer spectrum is the time average of the field at a probe site that is then averaged over many such sites across the whole system. By contrast, moments obtained in a neutron scattering experiment represent an instantaneous ensemble average over the Er moments in the system. In so far as time and ensemble averages are equivalent, and as long as the relaxation effects are not too severe, the average magnetic splitting in a Mössbauer spectrum should be a good measure of the average Er moment. We therefore tried a simple static model that used two Gaussian distributions of hyperfine fields to account for the line broadening and obtain the average magnetic splitting at each site. These static fits were as good as the dynamic ones (described below) up to about 6 K, above this temperature, dynamic fits were clearly superior. Below 6 K, the average hyperfine fields obtained in this manner were indistinguishable (within 1%) from those returned by the dynamic model. The simplest way to formally include the effects of dynamics

is to use a stochastic model¹⁰ in which the hyperfine field at an Er site is assumed to fluctuate randomly between $\pm B_{hf}$ with some average frequency ν . While this model yields excellent fits to the data, it yields zero net magnetization and, strictly speaking, describes a slowly relaxing paramagnetic system. For an ordered system relaxing between two exchange-split levels, we need to include the effects of unequal spin-up and spin-down level populations.⁸ In this model we have the hyperfine field due to static, $T=0$ K occupation of one level, (B_{hf}^0), an average fluctuation rate (ν), and an exchange splitting (Δ), which combined with the temperature, sets the relative occupations of the spin-up and spin-down levels. The thermally averaged hyperfine field is just the weighted average of the up and down contributions and is given by

$$B_{hf}(T) = B_{hf}^0 \times \tanh(\Delta/2T).$$

This model yields accurate fits to spectra up to 8 K (the highest temperature used here) and all of the Mössbauer results presented below are derived from these fits.

III. BASIC MAGNETIC CHARACTERIZATION

$\chi_{ac}(T)$ for Er_3Ge_4 (Fig. 2) exhibits a single clear cusp at $T_N = 7.2(1)$ K, in full agreement with previous reports.²⁻⁴ The out of phase signal (χ'') mirrors the χ' cusp with a weaker, more rounded peak, then rises sharply on cooling through 4 K. Fitting the high temperature section ($T \geq 40$ K) of the χ' data in Fig. 2 to a Curie-Weiss function yields a paramagnetic Curie temperature of $\theta_p = -4.40(2)$ K, consistent with antiferromagnetic ordering. The fit also yields an effective Er moment of $10.5(1) \mu_B$, somewhat larger than the expected paramagnetic moment of $9.58 \mu_B$, but consistent with values reported for ErGe_2 (Ref. 11) and ErGe_3 .¹²

Magnetization curves below T_N are clearly 'S'-shaped, with a marked increase starting at ~ 1 T (Fig. 3). This form weakens with increasing temperature, but is not lost until T_N . We could find no change in either the position or size of

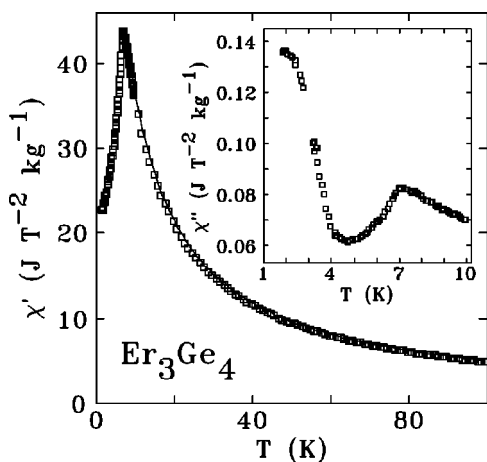


FIG. 2. Temperature dependence of the ac susceptibility (χ') for Er_3Ge_4 showing the cusp at $T_N=7.2(1)$ K. The solid line is a Curie-Weiss fit discussed in the text. The inset shows the out of phase (loss) response (χ'') which exhibits a peak at T_N , and then rises sharply below 4 K.

the break in slope that we could associate with the 3.5 K peak in the heat capacity,⁴ it therefore appears to be a field-driven change in the magnetic structure that is unrelated to any temperature-driven spin reorientation.² The magnetization curves were far from saturation in 6 T, however the maximum response at 2 K corresponds to an average moment of $5.2 \mu_B/\text{Er}$, a remarkably large fraction of the $7.0 \mu_B/\text{Er}$ possible according to the neutron diffraction data,² suggesting that an almost complete rearrangement of the antiferromagnetic spin structure occurs in only a few T. The relative ease with which the zero-field spin arrangement is destroyed reflects the rather weak exchange interactions in this system, and is consistent with the absence of evidence for the 4-K spin reorientation in the high-field data. However, the region below about 1 T was essentially linear at most temperatures, and a fit to data obtained below 0.6 T (so that the measurements at all temperatures were linear) yields the dc susceptibility (χ_{dc}) shown as circles in Fig. 4. χ_{dc}

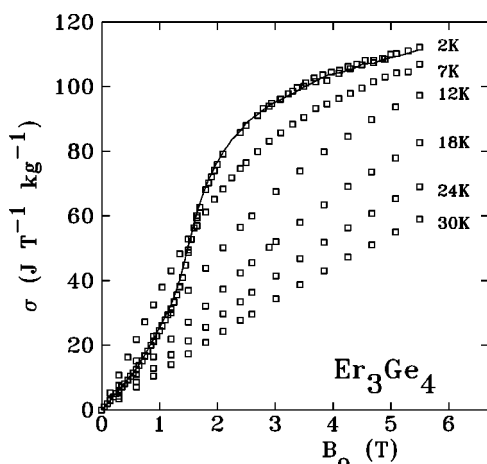


FIG. 3. Magnetization curves for Er_3Ge_4 at various temperatures. The 2-K curve has been highlighted with a solid line to make the S shape more obvious.

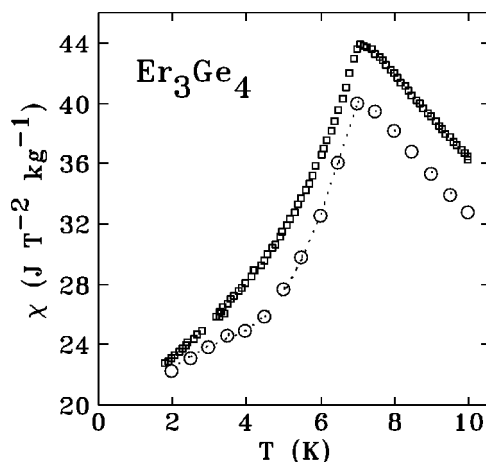


FIG. 4. Comparison of low-field ac susceptibility (χ') (squares) with the dc susceptibility (χ_{dc}) obtained below 0.6 T (circles) showing an inflection in $\chi_{dc}(T)$ at ~ 4 K. The dotted line is a guide to the eye.

shows behavior similar to that seen in χ' , with a peak at T_N . However, there is an apparent inflection at ~ 4 K, which might suggest that there is some change in magnetic behavior below T_N .

As will be clear from the ¹⁶⁶Er Mössbauer work that follows, the weak inflection in $\chi_{dc}(T)$ and the upturn in $\chi''(T)$ are the *only* indications of the 4-K spin reorientation² or the 3.5-K heat capacity feature^{3,4} that we have been able to observe in this study. Neither feature constitutes compelling evidence for any change in the intrinsic magnetic behavior of Er_3Ge_4 below T_N .

IV. ¹⁶⁶ER MÖSSBAUER RESULTS

The ¹⁶⁶Er Mössbauer spectrum of Er_3Ge_4 at 2.5 K (Fig. 5) shows that the two Er sites are fully resolved, exhibiting quite different magnetic hyperfine fields (B_{hf}), as expected from the earlier neutron diffraction data.² Four of the five magnetic lines clearly have two components (the central line results from the $0 \rightarrow 0$ hyperfine transition and is not affected by a magnetic hyperfine field). We find that the average fitted area of the more widely split pentet between 1.5 and 6 K is $65.2 \pm 2.3\%$ of the total area, fully consistent with the 2:1 ratio expected for Er in the $8f:4c$ sites. Since the observed area ratio is independent of temperature, we conclude that the recoil-free fractions (f factors) for the two sites are the same and so the spectral areas accurately reflect the crystallographic populations of the two Er sites. The clear agreement between the crystallographic site populations and the relative areas of the two subspectra permits unambiguous assignment of each component to Er atoms in specific crystallographic sites. The two hyperfine fields at 1.5 K are 654(1) T for the $8f$ site and 553(2) T for the $4c$ site, giving a field ratio of 1.183(5):1, which compares extremely well with the moment ratio of 1.15(2):1 determined by neutron diffraction at the same temperature.² These fields (and the neutron derived Er moments) are well below the 770 T and $9 \mu_B$ expected for free-ion Er in a pure $\frac{15}{2}$ ground state;¹³

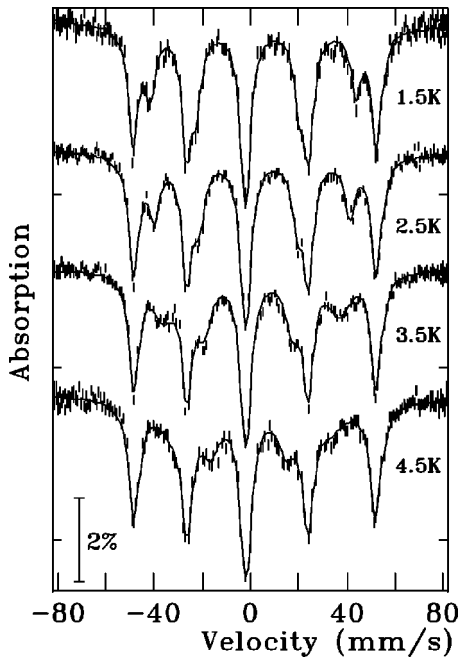


FIG. 5. ^{166}Er Mössbauer spectra of Er_3Ge_4 taken at temperatures well below T_N . The magnetic pentets from the two Er sites are clearly resolved, especially at 2.5 K. The very different temperature dependences of the splittings at the two sites are readily apparent. Solid lines are fits using the full Hamiltonian below 2.5 K, and a dynamic relaxation model above 2.5 K.

therefore there must be a substantial crystal-field induced admixture of other states, even at 1.5 K. Reduced Er moments appear to be a common feature of binary Er-Ge alloys.¹⁴

Visual inspection of the two components in the Mössbauer spectra in Fig. 5 reveals that they have very different temperature dependences, with the $8f$ subspectrum remaining essentially unchanged, while the $4c$ subspectrum collapses and broadens rapidly with increasing temperature. The results of fitting the spectra using the exchange-split relaxation model in Fig. 6 clearly show the very different thermal evolutions of the moments at the two Er sites. The observed magnetic splitting at the $8f$ site is essentially temperature independent, with significant relaxation effects setting in only at T_N as the exchange splitting is lost. Relaxation at the $8f$ site is so slow, even above T_N where the long-time average field must be zero, that the environment appears essentially static, and almost the full hyperfine splitting is observed through T_N . As a result, the fitted temperature dependence of the field at the $8f$ site does not provide a useful measure of the infinite-time-averaged moment of Er atoms at this site. By contrast, the field at the $4c$ site declines continuously and relaxation broadening appears above 2.5 K, well below T_N . Relaxation, while slow at the $4c$ site, is fast enough that a meaningful time-averaged hyperfine field can be derived, and this average field tracks the temperature dependence of the Er moment quite well (Fig. 6). For both sites, the spectra were initially fitted with ν as a free parameter; then it was constrained to a constant 1.5 GHz (determined from an average over the free fits) for the final refine-

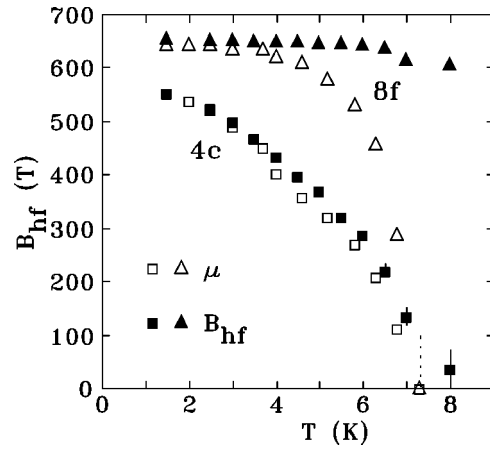


FIG. 6. Temperature dependence of the ^{166}Er hyperfine fields at the two Er sites in Er_3Ge_4 (solid symbols) derived from the relaxation model described in the text. For comparison, the Er moments derived from neutron diffraction data (Ref. 2) are shown as open symbols, scaled by a factor of $87.2 \text{ T}/\mu_B$ (see the text). Errors for the Mössbauer data generally lie well within the plotted points. The dotted line at 7.2 K marks T_N .

ment in order to reduce the effects of cross-correlations between ν and Δ . This constraint improved the stability of the fits, but had no discernible effect on the average field values. Fits to the spectra obtained between 5 and 8K, which exhibit more severe relaxation effects, are shown in Fig. 7.

The free-ion hyperfine field for $9\mu_B$ on Er is $770.5 \pm 10.5 \text{ T}$.¹³ There will be an additional contribution of

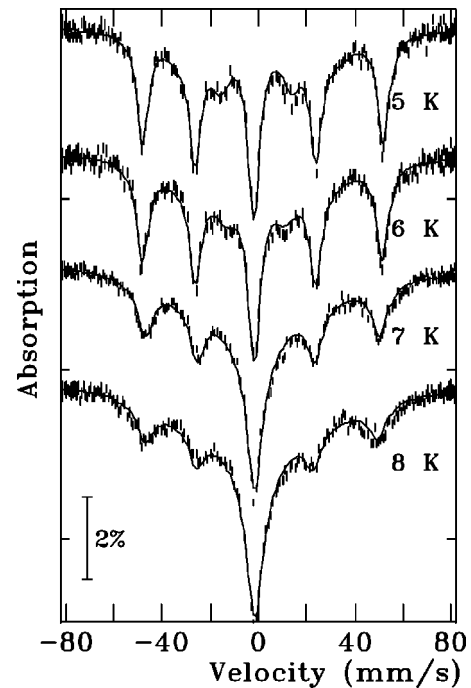


FIG. 7. ^{166}Er Mössbauer spectra of Er_3Ge_4 taken at temperatures around T_N . The inner pentet due to the Er- $4c$ site is already severely broadened, while the outer pentet associated with the Er- $8f$ site starts to broaden only above 6 K. The solid lines are fits using the relaxation model described in the text.

$\sim 14.1 \pm 2.1$ T from parent conduction electron polarization¹⁵ in a metallic environment, giving a total field of 784.6 ± 10.7 T and a moment to field conversion factor of 87.2 ± 1.2 T/ μ_B . The ratio between our average hyperfine field and the reported average Er moment² at 1.5 K is $88.3(5)$ T/ μ_B (where the error comes almost entirely from uncertainties in the neutron diffraction moments), in complete agreement with our estimated conversion factor. Taking the scaling factor as 87.2 T/ μ_B allows us to make a direct comparison between our measured hyperfine fields at the two Er sites and the two neutron diffraction derived moments² (open symbols in Fig. 6). The absolute agreement at 1.5 K is excellent. As noted above, the magnetic splitting at the $8f$ site shows very little temperature dependence, dropping slightly only above 6.5 K as relaxation effects start to become important at this site. However, even at 8 K the splitting of the $8f$ subspectrum is still over 90% of its value at 1.5 K (Fig. 6). Relaxation effects are so slow at the $8f$ site that we can derive no information about the temperature dependence of the Er moment at this site. By contrast, from 1.5 to 6.5 K the average hyperfine field at the $4c$ site tracks the reported temperature dependence of the Er moment at that site remarkably well, with one important difference: we see no evidence of the decrease at 4 K deduced from analysis of the neutron diffraction data² and attributed to the spin reorientation. The range of temperatures over which we obtain agreement between $\mu_{Er}(4c)$ and $B_{hf}(4c)$ clearly indicates that our analysis yields a meaningful estimate of the average Er moment at this site.

Given the excellent overall agreement and the enhanced precision provided by the ¹⁶⁶Er Mössbauer measurements compared with neutron diffraction, the absence of a break in slope in $B_{hf}(T)$ for the $4c$ site is highly significant. Within the uncertainty of our measurements ($<0.4\%$), there is no change in B_{hf} at the $4c$ site beyond the expected smooth thermal evolution. Our ¹⁶⁶Er Mössbauer spectra provide clear confirmation of the reduced Er moments and their distinct temperature dependences, but the spectra show no changes around 4 K that we could associate with a spin reorientation, or any other change in the intrinsic magnetic order.

V. DISCUSSION

It is clear that exchange interactions in this system are relatively weak ($T_N \sim 7$ K, $\theta_p \sim -4.4$ K), and the reduced Er moments point to significant crystal-field quenching ($\sim 27\%$ at the $4c$ site). In addition, the distinct ordering directions at the two Er sites coupled with the failure of the magnetization to saturate in 6 T, indicate that magnetocrystalline anisotropy plays a significant role in the magnetic ordering.

In order to develop some insight into the differences in both the moment magnitudes and their dynamics, we turn to the crystal-field environments of the two Er sites. Taking lattice parameters and atomic positions from neutron diffraction,² and using the BLOKJE program¹⁶ to determine the Wigner-Seitz cells and hence the nearest-neighbor environments, we find that both Er sites are fully coordinated by

TABLE I. Point symmetries and local environments for the two crystallographically distinct Er sites in Er₃Ge₄. Also shown are the crystal-field lattice sums to second order. To convert from A_{2m} (in units of Ka_0^{-2} , where a_0 is the Bohr radius) to the standard crystal-field parameters B_{2m} , multiply by $1.81 \times 10^{-3} \times Q_{Ge}$, where Q_{Ge} is the effective point charge on the neighbouring germanium ions.

Er site	Er ₁ (8f)	Er ₂ (4c)
Point symmetry	m..	m2m
First neighbors	8 Ge	7 Ge
Distances (Å)	2.96–3.04	2.83–3.14
Crystal field terms		
A_{20}	+246	–462
A_{21}^c	0	0
A_{21}^s	+5309	0
A_{22}^c	+230	–284
A_{22}^s	0	0

germanium atoms (Table I). We then used point-charge calculations to determine the crystal-field parameters at the two Er sites. We recognize that this is a severe approximation, especially in a metallic environment, but it should yield a reasonable description of the site symmetries and relative magnitudes of the terms within a given order. Parameters were calculated out to sixth order using orthogonal axes chosen coincident with the crystallographic axes. Values for the second order terms are shown in Table I.

The dominant contribution at the $4c$ site is clearly the diagonal A_{20} term, with the only off-diagonal contribution being down by almost a factor of 2. The negative sign for A_{20} taken with the measured easy c -axis ordering direction at this site² implies that the effective charge on the germanium ions is positive (within this point-charge approximation). By contrast, the sign of A_{20} at the $8f$ site is positive, indicating that the c -axis cannot be the easy axis at this site, however, the environment of the $8f$ site is dominated by off-diagonal terms, particularly A_{21}^s . We can eliminate this off-diagonal term by rotating our coordinate system [in a procedure analogous to identifying the principal axis system for the electric field gradient (efg) in a Mössbauer measurement] and thereby determine the easy axis predicted by our point-charge approximation. We obtain a canting angle of 40° away from c in the bc plane, which compares remarkably well with the reported value for this angle of $35.5(3)^\circ$.²

Er³⁺ is a Kramers ion with $J = \frac{15}{2}$ and so in the paramagnetic state the electronic energy levels comprise eight Kramers doublets. Using the results of our point charge calculations to second order, and assuming a standard 50% screening, yields splittings between the ground and first excited states of $\Delta E(4c) = 17.1$ K and $\Delta E(8f) = 47.5$ K. The full energy level diagram for the two sites, without the exchange splitting of ~ 7 K is shown in Fig. 8. It is clear that the overall splitting of the electronic levels is much greater at the $8f$ site than at the $4c$ site, and it is this larger level splitting that leads to the much slower relaxation of the Er³⁺ moment at the $8f$ site.

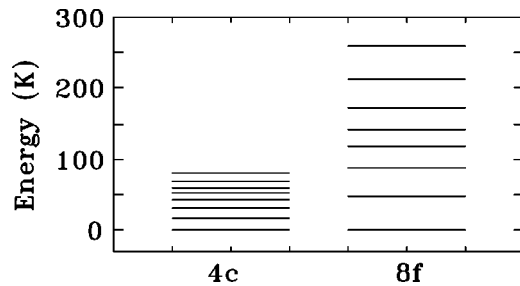


FIG. 8. Er^{3+} energy levels in Er_3Ge_4 for the $4c$ and $8f$ sites in Er_3Ge_4 .

The neutron diffraction data provided two signatures of the spin reorientation event at $\sim 4 \text{ K}^2$: (i) a change of somewhat less than 1° in the ordering direction of the moments on the $8f$ site, and (ii) a marked decrease in the moment on the $4c$ site on heating through $\sim 4 \text{ K}$. Even in an ideal system, ^{166}Er Mössbauer spectroscopy would not be able to resolve so small a change in ordering direction; however, it is clear from Fig. 6 that the second signature is well within the resolution of our data. There is no change in B_{hf} at the $4c$ site, beyond the expected smooth thermal evolution. We do not see any break in the temperature dependence. This conclusion is independent of the analysis model used, as both dynamic and static fits to the spectra yield identical average hyperfine fields, and so lead to the same result. Furthermore, the excellent agreement with the behavior of the moment at the $4c$ site both above and below the 4 K event (Fig. 6), coupled with the break in slope in the neutron diffraction data being close to the reported uncertainties would suggest that interpretation of the diffraction data in terms of a spin reorientation may be equivocal. Such a view would be more consistent with a heat capacity measurement that shows only a weak shoulder around 4 K ,³ and not with data exhibiting a large peak.⁴ The complexity of the Er-Ge binary phase diagram, and especially the fact that none of the binary phases

around Er_3Ge_4 melts congruently,¹⁷ makes some level of impurity almost inevitable. Indeed, none of our Er-Ge alloys were completely single-phase, and the sample of Er_3Ge_4 used in this study contained a ~ 5 -wt. % ErGe impurity (see Fig. 1). Our preliminary investigation of neighboring phases in this system¹⁴ has revealed that while ErGe does not lead to any interference, Er_2Ge_3 orders at $4.0 \pm 0.1 \text{ K}$. Er_2Ge_3 is extremely close in composition to Er_3Ge_4 (40 at. % Er vs. 43 at. %), and differing levels of Er_2Ge_3 impurities might account for the differences between the two calorimetric studies,^{3,4} and would not be inconsistent the claimed spin reorientation temperature.

VI. CONCLUSIONS

Er_3Ge_4 orders antiferromagnetically below $T_N = 7.2(1) \text{ K}$. In the ordered state, the Er atoms located on the two crystallographic Er sites have different moments and those moments exhibit distinct temperature dependences. These results are in complete agreement with previous neutron diffraction work.² However, we observe no significant changes in our data below T_N , and so find nothing to suggest the existence of a spin-reorientation transition around 4 K . The ordering directions of the moments at the two Er sites and their distinct temperature dependences can be understood in terms of the crystal field environments of the erbium ions in this structure.

ACKNOWLEDGMENTS

This work was supported by grants from the Natural Sciences and Engineering Research Council of Canada, Fonds pour la formation de chercheurs et l'aide à la recherche, Québec, and the Australian Research Council. The authors are grateful to Dr. G. Kennedy at the Ecole Polytechnique SLOWPOKE reactor facility, Montréal, where the activation of the ^{166}Ho sources used in this study was carried out.

¹O.Ya. Oleksyn and O.I. Bodak, *J. Alloys Compd.* **210**, 19 (1994).

²P. Schobinger-Papamantellos, O. Oleksyn, C. Ritter, C.H. de Groot, and K.H.J. Buschow, *J. Magn. Magn. Mater.* **169**, 253 (1997).

³Y. Janssen, E. Brück, F.E. Kayzel, F.R. de Boer, K.H.J. Buschow, O. Oleksyn, and P. Schobinger-Papamantellos, *J. Magn. Magn. Mater.* **177-81**, 1147 (1998).

⁴Y.Y. Chen, Y.D. Yao, Y.S. Lin, C.L. Chang, H.H. Hamdeh, and J.C. Ho, *Phys. Rev. B* **61**, 58 (2000).

⁵O. Zaharko, P. Schobinger-Papamantellos, W. Sikora, C. Ritter, Y. Janssen, E. Brück, F.R. de Boer, and K.H.J. Buschow, *J. Phys.: Condens. Matter* **10**, 6553 (1998).

⁶A.C. Larson and R.B. von Dreele, Los Alamos National Laboratory Report No. LAUR 86-748, 1994 (unpublished).

⁷J.A. Hodges, G. Jehanno, A. Schuhl, and Y. Berthier, *Hyperfine Interact.* **11**, 29 (1981).

⁸I. Nowik and H.H. Wickman, *Phys. Rev. Lett.* **17**, 949 (1966); M. Eibschütz, R.L. Cohen, and K.W. West, *Phys. Rev.* **178**, 572 (1969).

⁹W. Wiedemann and W. Zinn, *Phys. Lett.* **24A**, 506 (1967); P.C.M. Gubbens, A.M. van der Kraan, and K.H.J. Buschow, *Phys. Rev. B* **39**, 12 548 (1989).

¹⁰M. Blume and J.A. Tjon, *Phys. Rev.* **165**, 446 (1968).

¹¹O. Oleksyn, P. Schobinger-Papamantellos, C. Ritter, C.H. de Groot, and K.H.J. Buschow, *J. Alloys Compd.* **252**, 53 (1997).

¹²P. Schobinger-Papamantellos, G. André, J. Rodríguez-Carvajal, C.H. de Groot, and K.H.J. Buschow, *J. Alloys Compd.* **232**, 165 (1996).

¹³B. Bleaney, in *Handbook on the Physics and Chemistry of Rare Earths*, edited by K.A. Gschneidner, Jr. and L. Eyring (Elsevier, Amsterdam, 1988), Vol. 11, Chap. 77.

¹⁴D.H. Ryan, J.M. Cadogan, and R. Gagnon (unpublished).

¹⁵Y. Li, C. Carboni, J.W. Ross, M.A.H. McCausland, and D.St.P. Bunbury, *J. Phys.: Condens. Matter* **8**, 865 (1996).

¹⁶L. Gelato, *J. Appl. Crystallogr.* **14**, 151 (1982).

¹⁷*Binary Alloy Phase Diagrams*, edited by T.B. Massalski, J.L. Murray, L.H. Bennett, and H. Baker (American Society for Metals, Metals Park, OH, 1986).